Prepared for submission to JINST

A dump leakage calorimeter to measure the flux of high-energy electrons and photons

Antonios Athanassiadis[a,b] **Ties Behnke**[a] **Jonas Björklund Svensson**[a,1] **Oleksandr Borysov**[a,2] **Maryna Borysova**[a,2] **Lewis Boulton**[a] **Sarawit Chindaratchakul**[a,3] **Beate Heinemann**[a,b] **Louis Helary**[a] **Ruth Jacobs**[a] **Advait Kanekar**[a] **Jenny List**[a] **Tianyun Long**[a] **Tanguy Marsault**[a,4] **Felipe Peña**[a,b] **Stefan Schmitt**[a] **Sarah Schröder**[a,5] **Ivo Schulthess**[a,6] **Stephan Wesch**[a] **Matthew Wing**[a,c] **Jonathan Wood**[a]

[a] *Deutsches Elektronen-Synchrotron DESY, 22603 Hamburg, Germany*
[b] *Universität Hamburg, 22761 Hamburg, Germany*
[c] *University College London, London WC1E 6BT, United Kingdom*

E-mail: ivo.schulthess@desy.de

Abstract: We developed a novel apparatus based on a lead glass calorimeter that can measure the flux of high-energy electrons or photons. Our detector uses the electromagnetic shower leakage from the beam dump, where the particles are disposed of at the beamline's end. A prototype of such a calorimeter was set up at the FLASHForward experiment at DESY. We show that it can measure the electron bunch charge with precision and accuracy at the 10% and 3% level, respectively. Additionally, it is capable of determining the beam's position with a precision on the order of tens of micrometers. Finally, we show the applicability to the measurement of high-energy photons.

[1] Current address: Lund University, 22100 Lund, Sweden
[2] Current address: Weizmann Institute of Science, 7610001 Rehovot, Israel
[3] Current address: Mahidol University, 10400 Bangkok, Thailand
[4] Current address: CEA Paris-Saclay, 91190 Saclay, France
[5] Current address: Lawrence Berkeley National Laboratory, Berkeley, CA 94720, USA
[6] Corresponding author

1 Introduction

Accurately measuring high fluxes of high-energy photons is a general experimental challenge. Such photon beams can originate from future experiments and facilities, such as the LUXE experiment that is planned at the Deutsches Elektronen-Synchrotron DESY in Hamburg, Germany [1, 2]. LUXE aims to test quantum electrodynamics in the strong-field regime. The interaction of electron bunches from the European XFEL [3] with a high-intensity laser will produce pulses of $\mathcal{O}\left(10^9\right)$ photons with an energy spectrum of up to a few GeV. Similar photon sources could also be included in future circular or linear particle collider facilities such as the FCC-ee or LCF/CLIC/ILC, respectively [4].

These photon beams serve a key diagnostic tools for studying the strong-field quantum electrodynamics interaction and also offer promising opportunities as a probe in fixed-target experiments searching for new physics. The search for new phenomena beyond the standard model of particle physics through fixed-target or beam-dump experiments has recently regained particular interest. This is motivated by the absence of new physics signals at high-energy colliders and the theoretical expectation that weakly interacting particles, potential candidates for dark matter or mediators of hidden sectors, may be more effectively probed in high-intensity, low-background environments [5]. In these experiments, high-energy electrons or protons are dumped onto a solid target, where new long-lived particles can be produced and reconstructed via their decay products. Knowing the flux and properties of the beam impinging onto the target is critical. Various options exist to measure the flux of charged particles [6].

Current diagnostic systems for high-flux, high-energy photon beams typically use a target to partially convert the photon beam into electron-positron pairs, which can then be measured using a magnetic dipole spectrometer [7, 8]. However, this method has the disadvantage of disturbing the photon beam.[1]

In this paper, we describe a method for measuring the photon-beam flux without interfering with the beam during its transport. Our novel approach uses a lead-glass calorimeter to detect the electromagnetic shower leakage emerging from the beam dump, where the photons are ultimately absorbed. Although the beam is terminated at the dump, our measurement is non-invasive with respect to the beam's propagation and interaction up to that point. The shower leakage, which is the part of the electromagnetic shower that is not contained in the dump, is known to correlate with the photon beam flux [2]. This technique allows for flux monitoring without introducing any upstream disturbance to the beam or requiring additional components in the beamline.

Commissioning and testing of this detector is difficult because, to date, there is no running high-flux high-energy pulsed photon source that matches the requirements of the diagnostic system. To test the dump leakage calorimeter in such an environment, we exploited the similarities of the electromagnetic shower development in beam dumps for both photons and electrons. Specifically, we set up a prototype at the dump of the FLASHForward beam-driven plasma-wakefield experiment at DESY, where we could test the detector parasitically to the FLASHForward measurement campaigns [9].

[1] Furthermore, it requires a dipole magnet, a carefully selected converter target which has to be stable during operation, and a sizable particle detector that covers the spatial spread after the magnet.

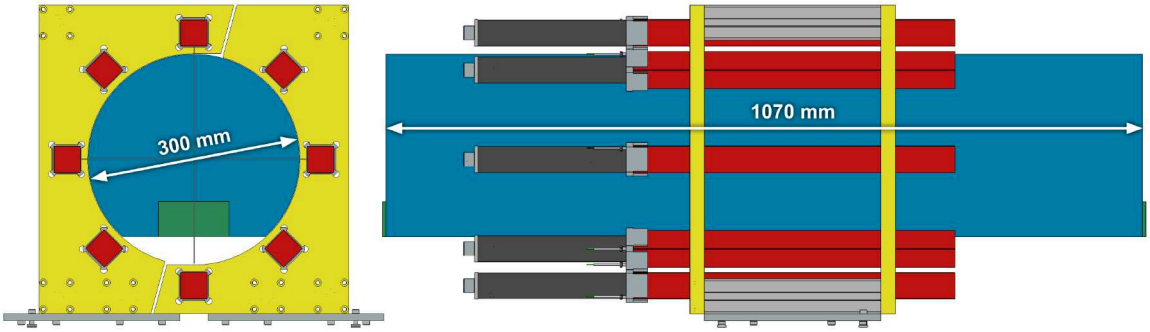

Figure 1: *CAD back view (left) and side view (right) of the FLASHForward beam dump (blue) with the dump leakage calorimeter consisting of lead-glass bars (red) that are read out with Photo-Multiplier Tubes (PMTs) that are mounted with a light guide inside a plastic housing (dark gray). Two scintillating tiles (green) are taped to the front and back face of the dump.*

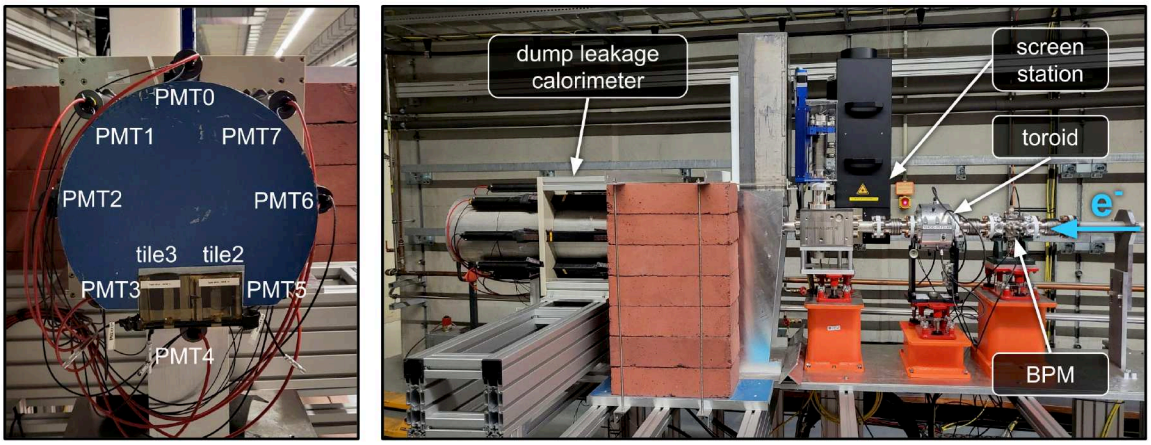

Figure 2: *Photos of the dump section of the FLASHForward experiment at DESY. (left) View of the backside of the dump. The eight PMTs are mounted around the dump and labeled PMT0 to PMT7. Two scintillating tiles with SiPMs, labeled tile2 and tile3, are taped to the dump below the beam axis. (right) Side view of the end of the beamline where the electrons enter from the right side. They first pass a beam position monitor (BPM), a toroid beam charge transformer to measure the bunch charge, and a screen station with a retractable scintillating screen to measure the transverse beam profile before exiting the vacuum beam pipe and hitting the dump.*

2 Setup

The FLASHForward experiment at the FLASH facility [10, 11] at DESY typically operates bunch charges up to 1 nC, corresponding to 6.2×10^9 electrons, at a rate of 10 Hz. The energy can be adjusted between 400 MeV and 1350 MeV with a relative full width at half maximum energy spread of $\lesssim 1\%$ with a linear chirp [9, 12]. These particle rates and energies are similar to those expected at the photon dump of the LUXE experiment [2]. Furthermore, the dump of the FLASHForward experiment is not obstructed by shielding and other elements, making it easily accessible for instrumentation.

The CAD design and photos of the detector setup are shown in figures 1 and 2, respectively. The dump is made of an aluminum-magnesium alloy (AlMg). It has a cylindrical shape with a length of 1070 mm and a diameter of 300 mm. A segment on the bottom side of the dump is removed to allow for a secure mounting. The calorimeter consists of eight lead-glass bars, which are coupled to Photo-Multiplier Tubes (PMTs), mounted around the dump. The lead-glass bars have a cross section of 38 mm × 38 mm, a length of 450 mm, and are of glass type TF1 [13] as used in the GAMS-2000 spectrometer [14]. The PMTs are of type XP1911/UV from Photonis SAS [15] and were used in the HERMES RICH detector [16]. The lead-glass bars and the PMTs are connected via optical wave guides made of plexiglas to transport the light. In addition to the lead-glass calorimeter modules, we mounted two scintillating tiles of size 60 mm × 60 mm × 5 mm that are optically connected to silicon photomultipliers (SiPMs) via wavelength-shifting fibers before and after the dump below the beam axis. The PMTs and SiPMs were electronically connected to a CAEN V1730 digitizer [17] that was controlled via a modified version of the CAEN Wavedump software [18]. The data acquisition was synchronized with the accelerator clock, using a delay to compensate for the position of the dump at the end of the facility. The digitizer acquired the full waveform of 1 µs - 2 µs for each channel and event with a 122 µV resolution and a sampling interval of 2 ns. Approximately 10^3 valid events per run were recorded.

In addition to the data from the dump leakage calorimeter, data from the accelerator beam diagnostics were recorded via the main accelerator control system [19, 20]. Three devices were used at the end of the beamline before the dump, which are indicated in figure 2. A button-type beam position monitor (BPM) allows measurement of the transverse beam position with a position noise of about 10 µm [21, 22]. A toroid beam charge transformer is used to precisely measure the bunch charge via passive induction and a resolution of about 1 pC [23]. Finally, a screen station with a retractable scintillating screen that is read by a camera system enables the determination of the shape and position of the beam [24]. The latter system has a resolution of 10.8 µm in x and 11.4 µm in y. It was used during a single data-taking campaign to ascertain the size of the beam spot. We determined a full width at half maximum size on the screen of (0.23 ± 0.01) mm in the horizontal direction and (0.63 ± 0.02) mm in the vertical direction for a 100 pC bunch charge. The screen was intermittently retracted during measurements, depending on the diagnostic requirements.

3 Measurements

The data presented here were obtained in several measurement campaigns. They are publicly available together with the analysis code [25, 26]. The accelerator electron energy was set to accommodate the requirements of the other users of the facility and could therefore not be specifically chosen or varied for this study.

The first successful campaign at FLASHForward in November 2023 allowed investigation of the position dependence of the signal described in section 3.3. The electron energy was 1050 MeV.

A later campaign in March 2024 with a beam energy of 1020 MeV is used to find the observable with the most linear response, explained in section 3.1 and enabled us to perform the charge calibration described in section 3.4.

The last campaign in April 2024 with a beam energy of 1200 MeV allowed comparison of the various sensor options described in section 3.2. It was used to validate the charge calibration and

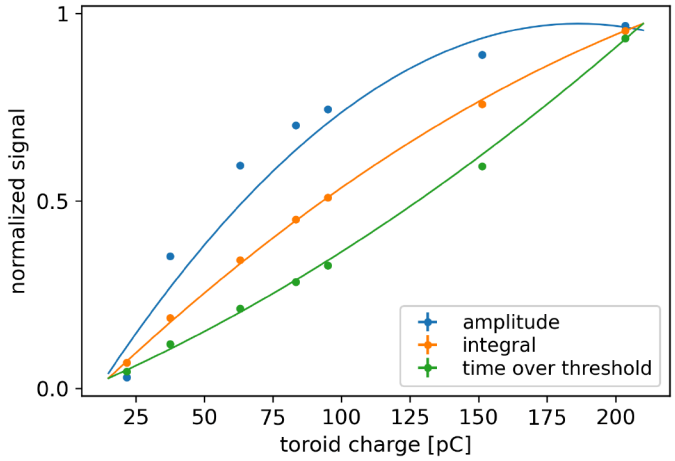

Figure 3: *Normalized signals of the recorded waveforms for various electron bunch charges. The three analysis methods that are compared are the waveform's amplitude (blue), integral (orange), and time over threshold (green). The data are fitted with quadratic polynomials.*

to determine the precision and accuracy of the bunch charge estimates. It is described in detail in section 3.4.

3.1 Observables

The analysis of the waveform (i.e. the signal as a function of time) typically focuses on one of the following three observables: the peak amplitude, the numerical waveform integral, or the time over threshold. A baseline was determined from data acquired before the signal arrived and was subtracted from all signals. To evaluate the time over threshold, a fixed threshold of 120 mV was used to avoid introducing a dependence on the signal amplitude. However, a relative threshold yields nearly identical results. Figure 3 shows the normalized observables of the three methods for comparison, together with the result of an orthogonal distance regression (ODR) [27] of a quadratic polynomial.[2] Given the evident non-linearity of the data and the absence of a physics-based model, we employed a quadratic function as the simplest non-linear approximation which empirically approximated the data. In our assessment, we used the waveform integral, which demonstrated better linearity, particularly in the higher charge range, along with a closer consistency with the quadratic model. As the model is purely empirical, statistical fit parameters, such as residual variance, are not interpreted as indicators of physical validity.

3.2 Sensors

One of the major limitations of the tested dump leakage calorimeter prototype is the non-linear signal response measured in the data-taking campaigns. In this first prototype, the signals of three sensor configurations were acquired. The first is the signal of the complete calorimeter, including the lead-glass bar, the light guide, and the PMT. In the second configuration, the lead glass was

[2]To account for uncertainties in both the independent and the dependent variable, we employed orthogonal distance regression (ODR). The uncertainties of the resulting parameters differ significantly from those obtained with ordinary least squares (OLS).

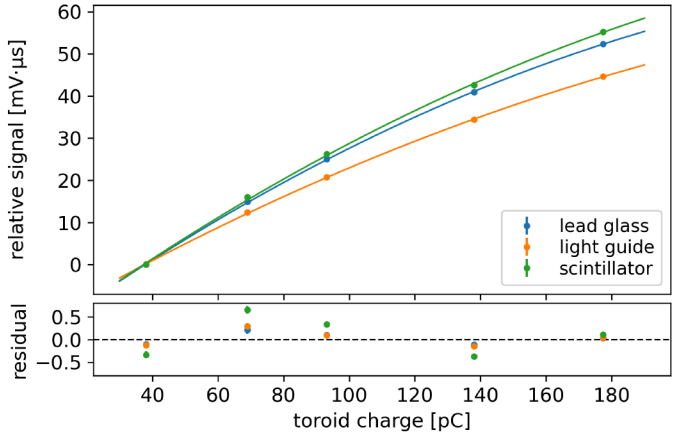

Figure 4: *Relative signal response of various sensor settings as a function of the electron bunch charge. The three settings shown are the response of a full calorimeter (blue), a configuration where the lead glass is optically separated (orange), and a scintillating tile (green). The data are fitted with quadratic polynomials. Displayed below are the residuals, representing the difference between the observed data and the fitted values.*

optically separated from the PMT with the light guide such that the Cherenkov light created in the lead glass could not reach the PMT. Finally, the signals from the plastic scintillators with the SiPMs were recorded.

The relative signal response in a charge scan is shown in figure 4. All signals were adjusted to 0 mV · µs for the lowest bunch charge of 38 pC for a relative comparison. The different sensor configurations show a similar response to increasing charges, i.e., a flattening of the curve. The lead-glass configuration was used for the analysis as it was employed in all measurement campaigns.

3.3 Position

The transverse position of the electron bunch can be steered with beamline magnets which are roughly 9 m upstream of the beam dump. A horizontal position scan was performed. The bunch charge for this measurement was (99 ± 1) pC. The signal integral as a function of the horizontal position is presented in figure 5 for PMT2, PMT6 (the ones horizontally opposite each other), and their average. An ODR of a straight line yields a slope of $(3.74 \pm 0.03)\,\mathrm{mV \cdot \mu s \cdot mm^{-1}}$ for PMT2, $(-3.69 \pm 0.09)\,\mathrm{mV \cdot \mu s \cdot mm^{-1}}$ for PMT6, and $(0.02 \pm 0.04)\,\mathrm{mV \cdot \mu s \cdot mm^{-1}}$ for the mean of the two. If the beam position was moved closer or farther from a calorimeter module, the signal increased or decreased, respectively. However, the mean of the two stayed constant over the tested range. This shows two important characteristics. The setup has the capability of resolving the position of the beam. The precision can be estimated from the uncertainty of the measured signal and the linear fit parameters by means of Monte Carlo uncertainty propagation, yielding a precision of 15 µm and 39 µm for PMT2 and PMT6, respectively. Moreover, the average signal remains unaffected by the beam's position and, consequently, insensitive to beam jitter. Thus, it is suitable for the analysis.

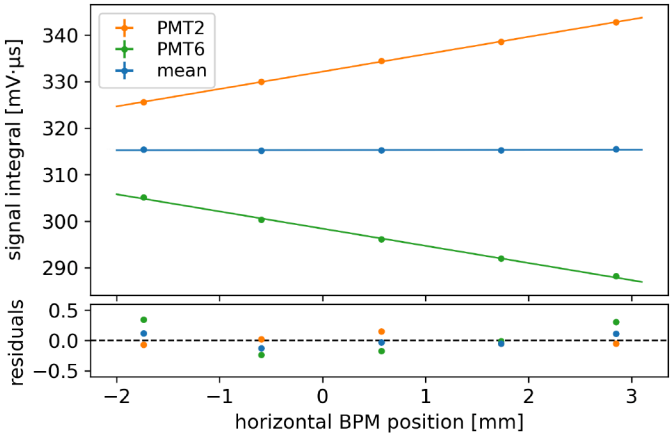

Figure 5: *Signal integral of PMT2 (orange), PMT6 (green), and the mean of the two (blue) as a function of the horizontal position measured by the last BPM before the dump along with a linear fit. The residuals are shown below, representing the difference between the observed data and the fitted values.*

3.4 Charge

Two separate measurement campaigns were conducted to investigate how effectively the dump leakage calorimeter can measure the bunch charge. In the March 2024 campaign, we calibrated the detector in an electron bunch charge range between 20 pC and 200 pC by relating the integral of the PMT signal to the bunch charge measured with the beamline toroid. The lower limit of the charge range is given by the working range of the BPM. At bunch charges above 200 pC, the signal response of the dump leakage calorimeter becomes too flat to produce reliable measurements. Moreover, the tested bunch charge regime corresponds to the approximate dynamic range of particle fluxes expected at the photon beam dump of the LUXE experiment, which will utilize the calorimeter.

The calibration measurements are shown in blue in figure 6. The data are interpolated with a quadratic function given in eq. (3.1)

$$I = C_E \times (p_2 Q^2 + p_1 Q + p_0) \,, \tag{3.1}$$

where C_E is a constant to account for the particle energy differences between the data-taking periods. For the calibration data set, it is fixed $C_E = 1$.

The second campaign served to validate the calibration. The electron energy was 1200 MeV. Given the difference, we used the data point of one charge setting to fit the constant C_E of eq. (3.1) while having the other parameters p_i fixed at the calibration measurement values. This is indicated in figure 6 by the charge measurement at 93 pC and the estimation curve in orange. The comparison of the toroid charge measurement with the estimated charge of the dump leakage calorimeter Q and its uncertainty σ_Q is presented in figure 7. It shows that both measurements are in good agreement. The uncertainties of the energy calibration and the charge estimation were estimated using Monte Carlo uncertainty propagation.

To assess systematic effects, the value of the energy calibration C_E is obtained for each measured charge setting and the other charges were determined. The results are summarized in figure 8. The

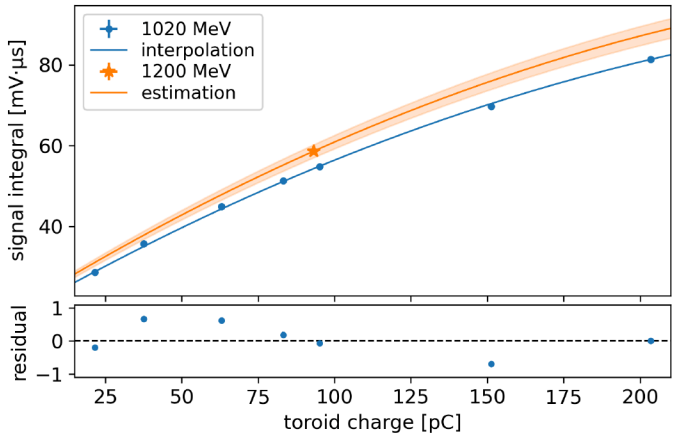

Figure 6: *Charge scan of the dump leakage calorimeter. It shows the measured signal integral of the waveform as a function of the electron bunch charge. The calibration measurements (blue ●) are fitted with the quadratic function given in eq. (3.1) with the parameter C_E fixed to one. One charge setting of the validation measurements (orange ★) has to be used to calibrate for the different electron beam energy. The estimation curve is shown in orange with its uncertainty band. The residuals are shown below, representing the difference between the observed data and the fitted values.*

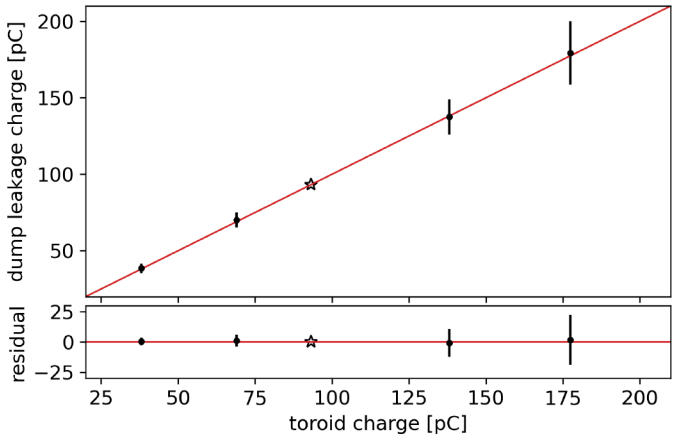

Figure 7: *Charge estimation from the dump leakage calorimeter when the* 93 pC *charge setting (indicated with ☆) is used for the energy calibration. The identity line is shown in red. The residuals are shown below, representing the difference between the observed data and the fitted values.*

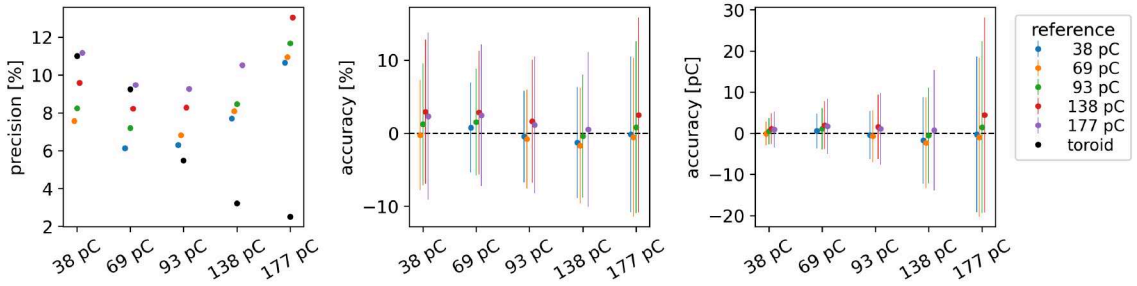

Figure 8: *Results of the bunch charge estimates of the dump leakage calorimeter. It shows the relative precision (left), the relative accuracy (middle), and the absolute accuracy (right) of the charge estimation. The various colors correspond to the different charge settings used for the energy calibration of the validation dataset. The black data represent the charge measurement of the toroid.*

left subfigure shows the relative precision σ_Q/Q, while the middle and right subfigures show the relative accuracy $(Q - Q_t)/Q_t$ and absolute accuracy $Q - Q_t$, respectively. Q_t is the charge measured by the toroid, which has a mean precision of 5 pC across all measurements. This reduced precision results from varying the bunch charge using a scraper, which likely introduces additional jitter through orbit fluctuations [28]. The results in figure 8 show that the precision is on the order of 10% while the accuracy is below 3%, regardless of the choice of energy calibration. However, they also indicate some systematic discrepancies that originate from the non-quadratic behavior of the calorimeter response, assumed in eq. (3.1), evident from the non-constant values of the precision and accuracy. The error bars in figures 7 and 8 reflect the total propagated uncertainty, including a systematic contribution from the energy calibration. The visible spread is smaller, as systematic effects do not induce point-to-point fluctuations.

4 Photon beam simulations

Even though the prototype of the dump leakage calorimeter was commissioned and tested at an electron beam dump, its main goal is to measure the flux of a pulsed photon beam. To show the applicability of the method, we performed simulations using the G4beamline tool v3.08 [29], which is based on Geant4 [30–32], with the QGSP_BERT physics list and its default settings. We compare the development of the electromagnetic shower and the energy deposited in the lead glass, i.e., the sum of the energy lost by all particle tracks that pass through the lead glass. The cases in which electrons or photons are disposed of in the dump were compared for a bunch with 6.24×10^8 particles, corresponding to an electron bunch with a charge of 100 pC. The beam energy was varied between 300 MeV and 3 GeV and for each particle type and energy, 25 trials with 10^5 macroparticles were simulated.

The results of the simulation are presented in figure 9. At energies below 500 MeV, the deposited energy for electrons and photons is the same within the statistical uncertainty of the simulation. At higher energy, both start to level off at slightly different rates, which leads to a lower energy deposition for a photon beam. This can be explained by the slight difference in the

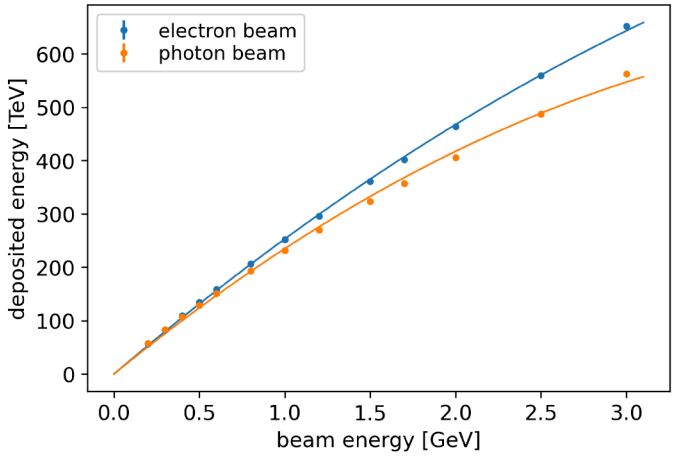

Figure 9: *Simulations of the deposited energy in a lead-glass bar of the calorimeter module as a function of the initial particle's energy for electrons (blue) and photons (orange). The statistical uncertainty of the simulation of less than 3% is smaller than the size of the data point. The solid lines are ordinary least-squares fits and serve only as a guide for the eyes.*

longitudinal shower profile of the two species and the geometrical acceptance of the lead glass. Nevertheless, the discrepancy only requires a recalibration for photons and does not pose an issue for the photon flux measurements in future experiments or facilities.

5 Conclusion

We presented a novel dump leakage calorimeter capable of operating in the high-flux, high-energy regime where diagnostics is challenging. It enables measurement of the electron or photon flux without affecting the beam before entering the dump. We demonstrated how a combination of detector channels located at different positions of the dump can be used to eliminate the position dependence and that we can resolve the position of the beam with a precision on the order of tens of micrometers. Furthermore, we showed that it can measure the number of electrons in a bunch with precision and accuracy on the 10% and 3% level, respectively, and that the concept is also applicable for high-energy photons. However, non-linearities of the calorimeter's response lead to systematic deviation of the bunch charge estimate that should be mitigated in the future upgrade of the detector.

6 Outlook

To minimize the non-linear signal response of the dump leakage calorimeter and for general improvements of the setup, a few items can be considered in a future upgrade:

- The position and orientation of the calorimeter modules were not fully optimized in this first prototype. Simulations should be performed to optimize the signal in the calorimeter so that shower leakage can be measured with the best sensitivity in the charge range of interest.

- Preliminary simulations and laboratory tests indicate that much of the signal in the calorimeter modules originates from scintillation in the light guide. The quenching of the scintillation light yield [33] together with a saturation of the PMT [34] probably causes the non-linear signal response when the bunch charge is increased. This could be mitigated by removing the light guide or by positioning the calorimeter module so that the particle flux through the light guide is reduced.

- Radiation damage must be considered, especially in the case of the LUXE dump leakage calorimeter. The lead glass used for this prototype cannot handle the radiation doses that are expected at LUXE in such a configuration. The more radiation hard lead glass TF101 could be used. Details must be discussed when the specific detector layout is worked out, such as the position of the calorimeter modules. An LED pulser is being developed to calibrate the calorimeter and monitor the darkening of the lead-glass bars.

- In a future experiment like LUXE, the photon spectrum will not be monochromatic but will span an energy range over several GeV. This will make the measurement more complicated and require more studies and tests.

Acknowledgments

The authors appreciate the technical support of Karsten Gadow, Sven Karstensen, Michelle Klotz, Beata Liss, Kai Ludwig, Frank Marutzky, Richie Nölling, Amir Rahali, Vladimir Rybnikov, and Andrej Schleiermacher. The experiment was performed at the beam-driven plasma-wakefield experiment FLASHForward at the FLASH facility of the Deutsches Elektronen-Synchrotron DESY in Hamburg, Germany. The AI-assisted tools OpenAI ChatGPT, Microsoft Copilot, and Writefull were used to help phrasing the text of this manuscript. This work was supported by the Swiss National Science Foundation under grant no. 214492 and by Helmholtz ARD, the Helmholtz IuVF ZT-0009 program.

Conflict of interest

The authors have no conflict of interest to disclose.

Author contributions

Contribution of all authors according to ANSI/NISO [35].

A. Athanassiadis: data curation (supporting); investigation (equal); methodology (equal); software (equal); validation (equal); writing – review & editing (supporting). **T. Behnke:** writing – review & editing (supporting). **J. Björklund Svensson:** investigation (supporting); writing – review & editing (supporting). **O. Borysov:** conceptualization (equal); writing – review & editing (supporting). **M. Borysova:** conceptualization (equal); writing – review & editing (supporting). **L. Boulton:** investigation (supporting); writing – review & editing (supporting).

S. Chindaratchakul: formal analysis (supporting); investigation (supporting); software (supporting); visualization (supporting); writing – review & editing (supporting). **B. Heinemann:** writing – review & editing (supporting). **L. Helary:** conceptualization (supporting); data curation (supporting); formal analysis (supporting); funding acquisition (equal); investigation (equal); methodology (equal); project administration (equal); software (equal); supervision (equal); validation (equal); writing – review & editing (equal). **R. Jacobs:** investigation (supporting); writing – review & editing (supporting). **A. Kanekar:** investigation (supporting); writing – review & editing (supporting). **J. List:** writing – review & editing (supporting). **T. Long:** investigation (supporting); writing – review & editing (supporting). **T. Marsault:** investigation (equal); writing – review & editing (supporting). **F. Peña:** investigation (supporting); writing – review & editing (supporting). **S. Schmitt:** resources (equal); writing – review & editing (supporting). **S. Schröder:** investigation (supporting); writing – review & editing (supporting). **I. Schulthess:** data curation (lead); formal analysis (lead); funding acquisition (equal); investigation (equal); methodology (lead); project administration (equal); software (equal); supervision (equal); validation (equal); visualization (lead); writing - original draft (lead); writing – review & editing (equal). **S. Wesch:** investigation (supporting); writing – review & editing (supporting). **M. Wing:** writing – review & editing (supporting). **J. Wood:** investigation (supporting); writing – review & editing (supporting).

Data availability

The data and analysis that support the findings of this study are openly available [25, 26].

References

[1] H. Abramowicz, U.H. Acosta, M. Altarelli, R. Assmann, Z. Bai, T. Behnke et al., *Conceptual Design Report for the LUXE Experiment*, *The European Physical Journal Special Topics* **230** (2021) 2445 [2102.02032].

[2] LUXE Collaboration, H. Abramowicz, M. Almanza Soto, M. Altarelli, R. Aßmann, A. Athanassiadis et al., *Technical Design Report for the LUXE experiment*, *The European Physical Journal Special Topics* (2024) .

[3] R. Abela, A. Aghababyan, M. Altarelli, C. Altucci, G. Amatuni, P. Anfinrud et al., *XFEL: The European X-Ray Free-Electron Laser - Technical Design Report*, 2006. 10.3204/DESY_06-097.

[4] I. Schulthess and F. Meloni, *New Physics Search with the Optical Dump Concept at Future Colliders*, Mar., 2025. 10.48550/arXiv.2503.20996.

[5] J. Beacham, C. Burrage, D. Curtin, A. De Roeck, J. Evans, J.L. Feng et al., *Physics beyond colliders at CERN: Beyond the Standard Model working group report*, *Journal of Physics G: Nuclear and Particle Physics* **47** (2020) 010501.

[6] T. Lensch, D. Lipka, R. Neumann and M. Werner, *Comparison of Different Bunch Charge Monitors Used at the ARES Accelerator at DESY*, in *Journals of Accelerator Conferences Website*, (Saskatoon, Canada), pp. 169–173, JACoW Publishing, 2023, DOI.

[7] K. Fleck, N. Cavanagh and G. Sarri, *Conceptual Design of a High-flux Multi-GeV Gamma-ray Spectrometer*, *Scientific Reports* **10** (2020) .

[8] N. Cavanagh, K. Fleck, M.J.V. Streeter, E. Gerstmayr, L.T. Dickson, C. Ballage et al., *Experimental characterization of a single-shot spectrometer for high-flux, GeV-scale gamma-ray beams*, *Physical Review Research* **5** (2023) .

[9] R. D'Arcy, A. Aschikhin, S. Bohlen, G. Boyle, T. Brümmer, J. Chappell et al., *FLASHForward: Plasma wakefield accelerator science for high-average-power applications*, *Philosophical Transactions of the Royal Society A: Mathematical, Physical and Engineering Sciences* **377** (2019) 20180392.

[10] S. Schreiber and B. Faatz, *The free-electron laser FLASH*, *High Power Laser Science and Engineering* **3** (2015) e20.

[11] B. Faatz, E. Plönjes, S. Ackermann, A. Agababyan, V. Asgekar, V. Ayvazyan et al., *Simultaneous operation of two soft x-ray free-electron lasers driven by one linear accelerator*, *New Journal of Physics* **18** (2016) 062002.

[12] C.A. Lindstrøm, J. Beinortaitė, J. Björklund Svensson, L. Boulton, J. Chappell, S. Diederichs et al., *Emittance preservation in a plasma-wakefield accelerator*, *Nature Communications* **15** (2024) 6097.

[13] Lytkarino Optical Glass Factory, JSC, "TF1 glass type."

[14] F. Binon, V. Buyanov, S. Donskov, P. Duteil, M. Gouanere, A. Inyakin et al., *Hodoscope multiphoton spectrometer GAMS-2000*, *Nuclear Instruments and Methods in Physics Research Section A: Accelerators, Spectrometers, Detectors and Associated Equipment* **248** (1986) 86.

[15] PHOTONIS S.A.S, *Photomultiplier Tubes Catalogue*, 2007.

[16] HERMES Collaboration and D. Ryckbosch, *The HERMES RICH detector*, *Nuclear Instruments and Methods in Physics Research Section A: Accelerators, Spectrometers, Detectors and Associated Equipment* **433** (1999) 98.

[17] CAEN SpA, *DS3153 - 730 Digitizer Family 16/8 Channel 14-bit 500 MS/s Data Sheet*, Nov., 2019.

[18] S. de Jong, "CAEN-v1730-DAQ." `https://github.com/samdejong86/CAEN-v1730-DAQ`, June, 2023.

[19] O. Hensler and K. Rehlich, *DOOCS: A distributed object oriented control system*, in *15th Conference on Charged Particle Accelerators*, pp. 308–315, 1996.

[20] S. Karstensen, S. Bohlen, J. Dale, M. Dinter, J. Müller, P. Niknejadi et al., *FLASHForward: DOOCS Control System for a Beam-Driven Plasma-Wakefield Acceleration Experiment*, *Proceedings of the 9th Int. Particle Accelerator Conf.* **IPAC2018** (2018) 3 pages, 1.403 MB.

[21] D.M. Treyer, R. Baldinger, R. Ditter, B. Keil, W. Koprek, G. Marinkovic et al., *Design and Beam Test Results of Button BPMs for the European XFEL*, in *International Beam Instrumentation Conference IBIC 2013*, (Oxford, UK), pp. 723–726, 2013.

[22] N. Baboi, H.T. Duhme and B. Lorbeer, *Beam Position Monitoring of Multi-bunch Electron Beams at the FLASH Free Electron Laser*, .

[23] M. Werner, R. Neumann, J. Lund-Nielsen and N. Wentowski, *Sensitivity Optimization Of The Standard Beam Current Monitors For XFEL and FLASH II*, in *European Workshop on Beam Diagnostics and Instrumentation for Particle Accelerators DIPAC2011*, (Hamburg, Germany), pp. 197–199, 2011.

[24] C. Wiebers, M. Holz, G. Kube, D. Noelle, D. Nölle and G. Priebe, *Scintillating Screen Monitors for Transverse Electron Beam Profile Diagnostics at the European XFEL*, in *International Beam Instrumentation Conference IBIC 2013*, (Oxford, UK), pp. 807–810, 2013.

[25] I. Schulthess, "Ivoschulthess/dumpLeakageCalorimeter: V1.0." Zenodo, 2025. 10.5281/zenodo.15281065.

[26] I. Schulthess, A. Athanassiadis and L. Helary, *Raw data of the measurements and simulations of the dump leakage calorimeter*, June, 2025. 10.5281/zenodo.14029383.

[27] P.T. Boggs and J.R. Donaldson, *Orthogonal Distance Regression*, *NIST Publications* **89** (1989) 20.

[28] S. Schröder, K. Ludwig, A. Aschikhin, R. D'Arcy, M. Dinter, P. Gonzalez et al., *Tunable and precise two-bunch generation at FLASHForward*, *Journal of Physics: Conference Series* **1596** (2020) 012002.

[29] T. Roberts and Muons, Inc., "G4beamline Users Guide 3.08." https://www.muonsinc.com/Website1/Muons/G4beamlineUsersGuide.pdf, Aug., 2022.

[30] S. Agostinelli, J. Allison, K. Amako, J. Apostolakis, H. Araujo, P. Arce et al., *Geant4—a simulation toolkit*, *Nuclear Instruments and Methods in Physics Research Section A: Accelerators, Spectrometers, Detectors and Associated Equipment* **506** (2003) 250.

[31] J. Allison, K. Amako, J. Apostolakis, H. Araujo, P. Arce Dubois, M. Asai et al., *Geant4 developments and applications*, *IEEE Transactions on Nuclear Science* **53** (2006) 270.

[32] J. Allison, K. Amako, J. Apostolakis, P. Arce, M. Asai, T. Aso et al., *Recent developments in Geant4*, *Nuclear Instruments and Methods in Physics Research Section A: Accelerators, Spectrometers, Detectors and Associated Equipment* **835** (2016) 186.

[33] J.B. Birks, *Scintillations from Organic Crystals: Specific Fluorescence and Relative Response to Different Radiations*, *Proceedings of the Physical Society. Section A* **64** (1951) 874.

[34] Hamamatsu Photonics K.K., *PHOTOMULTIPLIER TUBES Basics and Applications*, Hamamatsu Photonics K.K., fourth edition ed. (2017).

[35] NISO CRediT Working Group, *ANSI/NISO Z39.104-2022, CRediT, Contributor Roles Taxonomy*, Feb., 2022. 10.3789/ansi.niso.z39.104-2022.